changes. The density of this current is greatest closest to the x-axis, and this is shown by the greater density of lines there.

An equation for $\rho H \phi$ was obtained from Ryder (*2*):

$$\rho H_\phi = K_1 \sin \frac{\pi}{2} p \, (1 - \zeta) \cdot e^i \left(\frac{\pi}{2} p\eta - \omega t - \frac{\pi}{2} p \right)$$

where η and ζ are the radial and angular coordinates, respectively, ω is the angular velocity, and p is an integer for each harmonic. The real part of this equation was used with p set equal to 1:

$$R_e \, (\rho \, H_\phi) = K_1 \cos \left(\frac{\pi}{2} \zeta \right) \sin \left(\frac{\pi}{2} \eta - \omega t \right)$$

This equation was made equal to a constant, and a different value was used for each streamline in a nest.

$$K_2 = \cos \left(\frac{\pi}{2} \zeta \right) \sin \left(\frac{\pi}{2} \eta - \omega t \right)$$
$$K_2 = .05, .15, \cdot \cdot \cdot \cdot .95$$

where the outermost streamline of each half cycle is determined by the smallest constant. The spheroid coordinates ζ and η are related to the 2-*D* cartesian coordinates ρ and χ by

$$\rho = f \, [(1 - \zeta^2)(\eta^2 - 1)]^{1/2}$$
$$x = f \cdot \zeta \cdot \eta$$

These equations hold for a resonant spheroidal antenna whose interfocal distance ($2f$) is $\lambda/2$. The points along a streamline are computed at approximately equal spacing through an iterative process. First, ζ is incremented, then η is computed, followed by ρ, χ, and the distance from the preceding point. If the distance between points is within set limits, the new point is stored; otherwise, the increment in ζ is changed by the ratio of the desired distance to the calculated distance, and the above procedure is repeated. When all the points for one streamline have been calculated, they are transformed into SC 4020 control words and placed on magnetic tape.

Both the time increment between each frame and the distance for each half-cycle can be calculated by adding the proper value to η before transforming to the ρ,χ coordinate system used by the plotter.

My investigation shows that, for many curves, it may be better to plot curved lines by means of touching dots rather than by line segments. The pictures have a smoother appearance, and the machine time for calculating these does not seem to be excessive. In the examples shown, the dots are two raster counts apart. About 20 seconds on the 7094 computer was used to produce the tape for each picture.

The IBM 7094 computed this pattern at 96 different positions in the cycle. The tape represented one cycle over 4 seconds of movie at 24 frames per second. This tape was processed eight times by the SC 4020 to create 30 seconds of 16-mm film.

The movie started with the title, credits, and one scene of text. This was followed by displaying the focal points, drawing an ellipse, and rotating it to show that three dimensions were present. A generator symbol in the center and the dark fringe on the surface, proportional to charge, were added. This was followed by three main scenes. First, the radiated field was shown (Figs. 1 and 2). Then the field was frozen, and two rulers were used to show that the distance between the focal points of the ellipse was equal to one-half wavelength. Finally, segments were added to the streamlines. These segments moved around the streamlines to indicate the direction of motion of the displacement field. This was followed by "the end" in block letters. All scenes including the lettering were generated by the computer. The method of using streamlines to show the magnetic field and moving segments to show the displacement current could be applied to a number of field configurations in electromagnetics.

One of the main purposes behind the film was to explain a rather complex subject to the viewer regardless of his mathematical background. For example, the increased phase velocity of the near field can be seen very clearly. In conclusion, the technique should serve as an accessory in promoting understanding in both classrooms and laboratories.

BRENTON R. GROVES
Goodyear Aerospace Corporation, Akron, Ohio 44315

References and Notes

1. I. L. Finkle, *Science* **148**, 1541 (1965); K. C. Knowlton, *ibid.* **150**, 1116 (1965); G. A. McCue and J. D. O'Keefe, *ibid.* **151**, 839 (1966); A. C. Wahl, *ibid.*, p. 961.
2. These equations are explained in detail by R. M. Ryder, *J. Appl. Phys.* **13**, 327 (1942).
3. I thank Prof. J. D. Cowan, Jr., Prof. E. Kennaugh, and D. Shupe of the electrical engineering department of Ohio State University, the Numerical Computation Laboratory of Ohio State University, the National Committee for Electrical Engineering Films, and Educational Services, Inc., for help in this work.

1 December 1966

Ratio of Blue to Red Light: A Brief Increase Following Sunset

Abstract. *Visible spectra of solar radiation were recorded during sunset. With the development of twilight, there was an expected decrease in the blue-to-red ratio; but directly upon setting of the sun there was a sharp rise in this ratio (due to the predominance of skylight) which attenuated rapidly to follow the pattern that it had previously taken.*

Microclimatology has made tremendous strides in elucidating the physical parameters of the environment to which the plant is exposed, but, of all the factors comprising the above-ground environment, light (and its measurement) has posed the most elusive problems (*1*). This relates not only to physical factors, such as simultaneous variation in intensity and spectral composition (*2*), but also to the lack of instruments capable of recording significant data. The thermopile or photoelectric cell can produce a simple integration of the variables of light, but such readings have limited relevance to photobiological responses which are largely

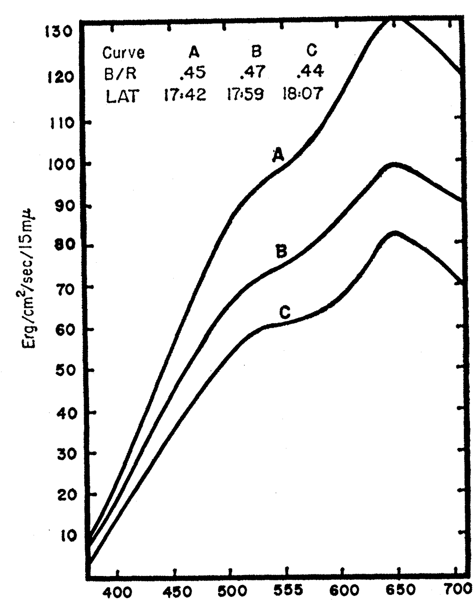

Fig. 1. These data were recorded 23 miles (37 km) west of Washington, Kansas, at an elevation of about 1300 feet. Sunset was apparent (sun barely above horizon). Time was recorded in local apparent time (*LAT*). The integrating sphere was directly facing the sun. Note that after sunset had occurred the visible spectrum assumed the same general shape as before sunset. Compare with curves D and E, Fig. 2. Numbers on the ordinate must be multiplied by 10^2.

photochemical. Most important is the number of photons the pigment receptors are receiving from any one region of the solar spectrum. Only recently have instruments capable of this kind of measurement become available (*3*).

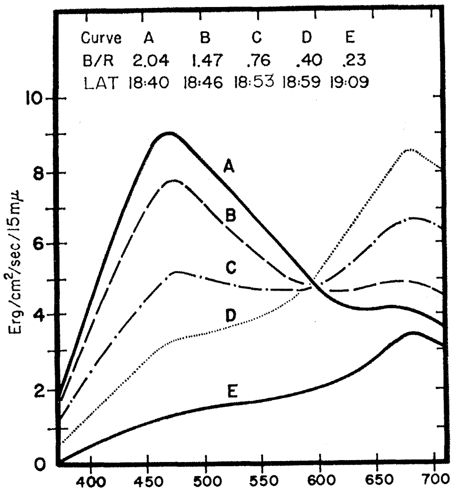

Fig. 2. Data show continuation of the sunset of Fig. 1. (A) Sun was exactly behind horizon; (B) sun had been down 5 minutes; (C) 13 minutes; (D) 21 minutes; and (E) 30 minutes. Data for all curves were recorded with the integrating sphere directly facing the sun or the sunset. Numbers on the ordinate must be multiplied by 10^2.

Excellent reviews describing the light environment and energy exchange have been written by Gates (*4*). Summaries of the applications of microclimatological data to studies of plants in controlled environments are also available (*5*).

Solar radiation is attenuated in the atmosphere by molecular (Rayleigh) scattering and by large-particle (Mie) scattering due to dust, water droplets, and other particles in the size range of the wavelength of the incoming radiation. Gates (*2*) shows the variation in spectral distribution of solar rays as a function of wavelength at different altitudes and at different air masses (densities). These data show that with an increase in atmospheric density, there is a decrease in the blue-to-red ratio (B/R).

A study of the quality of light in natural environments was made at Colorado State University. Data were recorded by a recently developed wedge filter spectroradiometer, in which a column of integrated light is transmitted first through an integrating sphere and a wedge filter, and then intercepted by a photomultiplier tube. The photomultiplier tube is most sensitive in the blue region of the spectrum, so that other regions must have electronic compensation. The instrument translates the transmitted relative energy onto recording strip charts. It is accurate from 400 to 700 mμ and is calibrated by comparison with a calibrated Eppley thermopile and narrow-band interference filters (*6*).

In this report, data relative to the quality of light during sunset are presented (the phenomenon described here is also apparent during sunrise). As the sun approaches the horizon, the rays must travel through a greater distance of air, which results in a reduction in both intensity and the blue-to-red ratio. This phenomenon is clearly apparent in the red of a sunset. Figures 1 and 2 show spectra recorded during a sunset near Washington, Kansas; Fig. 3, the marked shift in the B/R ratio during development of twilight on (A) Mt. Evans, Colorado (8 August 1965), at an elevation of 14,280 feet (4352 meters); and (B) at Washington, Kansas (26 August 1965), at an elevation of about 1300 feet (396 meters). Curve A shows the B/R ratio with the opening of the integrating sphere horizontal to the earth's surface, and curve B shows this ratio with the opening of the sphere directly facing the sun.

It can be noted from Fig. 2 that immediately after sunset (0 elevation) the absolute amount of blue is decreasing, as is the amount of blue relative to the red, whereas the absolute amount of red is increasing (for about 20 minutes). In Fig. 3 (typical of several observations), the B/R ratio is shown to decrease just before sunset, as expected. As the sun sets, however, a sharp rise in the blue is indicated, with a subsequent decrease at an equally rapid rate, the red again becoming predominant.

The explanation for this change of ratio is that, before the sun sets, it is directly illuminating the integrating sphere (or the plant). Skylight is also being recorded, but the direct solar radiation is dominant. When the sun sets, however, only the blue scattering of skylight is recorded, thus accounting for the sudden rise in blue; a blue increase may also be observed during totality of a solar eclipse (*7*). This skylight deepens with red scattering as the solar rays traverse a rapidly increasing depth of atmosphere, which results

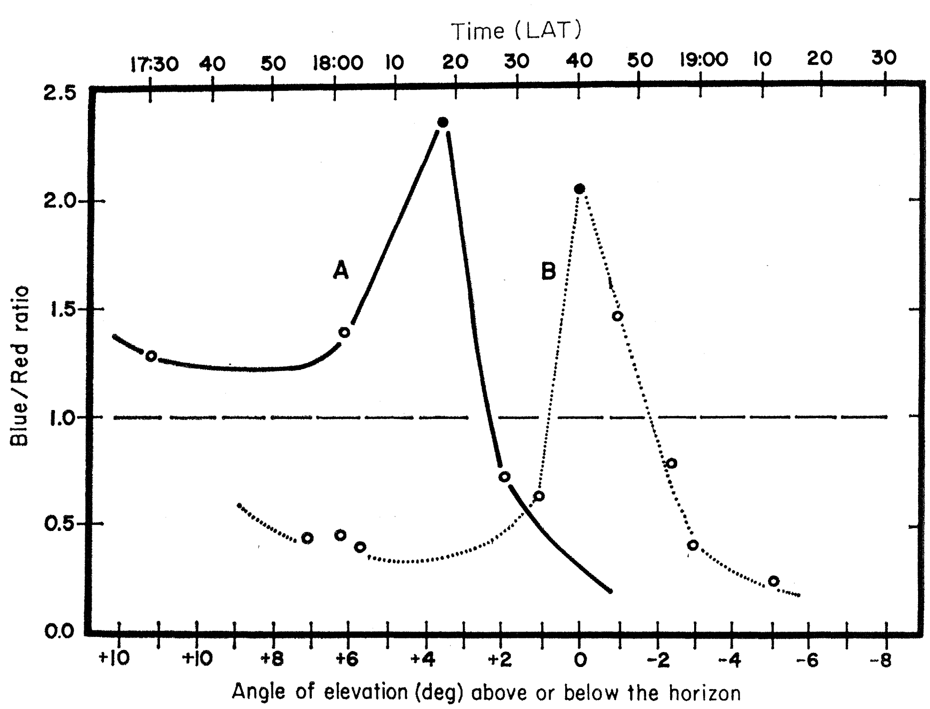

Fig. 3. Blue-to-red ratios of sunset at two different locations. (A) Mt. Evans, Colorado, 8 August 1965. Opening of the integrating sphere was horizontal to the earth's surface. (B) Washington, Kansas, 26 August 1965. Integrating sphere was directly facing the sun (see Figs. 1 and 2). (Sunset at Mt. Evans took place earlier than sunset at Washington, Kansas, even though the dates suggest that the latter should have occurred first. The reason for the earlier sunset at Mt. Evans is that at this location the sun set behind a rather large hill instead of on the horizon as it did in Kansas. The angle in degrees above the horizon applies only to the Kansas data and refers to the upper limb of the sun.)

in a greater percentage of red to blue. Whether this shift in blue at sunset has any biological or other significance remains to be seen.

TERRANCE B. JOHNSON
FRANK B. SALISBURY*
GERALD I. CONNOR

Department of Botany and Plant Pathology, Colorado State University, Fort Collins 80521

References and Notes

1. G. C. Evans, *J. Ecol.* **44**, 391 (1956).
2. D. M. Gates, *Science* **151**, 523 (1966).
3. K. H. Norris, *Annu. Meeting Amer. Soc. Agr. Eng.* (1963), paper No. 63, p. 329; M. W. Coulter *et al.*, *Proc. Amer. Soc. Hort. Sci.* **87**, 563 (1965); R. J. Downs, K. H. Norris, W. A. Bailey, H. H. Kleuter, *ibid.* **85**, 663 (1964); F. G. Teubner, S. H. Wittwer, R. S. Lindstrom, H. Archer, *ibid.* **82**, 619 (1963); T. H. Bulpitt, M. W. Coulter, K. C. Hamner, *Appl. Opt.* **4**, 793 (1965); R. C. Hirt, R. G. Schmitt, N. D. Searle, A. P. Sullivan, *J. Opt. Soc. Amer.* **50**, 706 (1960).
4. D. M. Gates, *Semicentennial Celebration Proc.* (Univ. of Michigan, Ann Arbor, 1959), p. 31; *Proc. Third Symposium of Remote Sensing of Environment* (Univ. of Michigan, Ann Arbor, 1965), p. 573; *Science* **151**, 523 (1966).
5. L. T. Evans, *Environmental Control of Plant Growth* (Academic Press, New York, 1963); J. P. Hudson, *Control of Plant Environment* (Academic Press, New York, 1957); F. W. Went, *The Experimental Control of Plants* (Chronica Botanica Co., Waltham, Mass., 1957).
6. T. B. Johnson, thesis, Colorado State University (1966).
7. W. E. Sharp, J. W. F. Lloyd, S. M. Silverman, *Appl. Opt.* **5**, 787 (1966).
8. Supported by NASA grant Ns G 78-60 and by a NASA trainee fellowship to T.B.J.
* Present address: Plant Science Department, Utah State University, Logan 84321.

7 February 1967

Pollen Diagrams from Sub-Arctic Central Canada

Abstract. *Peat from Keewatin and Manitoba contained macrofossil and palynological evidence of former latitudinal movements of the forest-tundra boundary in response to the changing location of the mean summer position of the Arctic front. Radiocarbon dating demonstrates the synchroneity of these climatic changes with those registered in northwest Europe during the past 6000 years.*

The work of Bryson, Irving, and Larsen (*1*) on the stratigraphy of the forest-tundra ecotone in Canada demonstrated the northward extension of continuous forest beyond its present limit during postglacial time. These conclusions are now supported and amplified by palynological evidence from two peat bogs which contain records of vegetational and climatic change.

The two sites lie in the northern part of the Boreal forest and at the tundra edge, locations which should have recorded past movements of the forest limit in response to climatic change. Bryson (*2*) has demonstrated the coincidence of the northern limit of continuous forest in central Canada with the average summer position of the Arctic frontal zone. He suggests that past movements of the tree line in this area have been in response to changes in the climatic boundary between Arctic air in the north and air masses of Pacific or tropical origin in the south. I have attempted to estimate the position of the Arctic front from the forest history derived from the pollen diagrams, especially the Ennadai pollen diagram. Its ecotonal location and sphagnum peat constitution make it more sensitive to climatic changes than Lynn Lake, the latter being in a more "complacent" position in the middle of the Boreal forest. The Lynn Lake diagram provides confirmation of the major changes registered at Ennadai.

Peat monoliths were collected from Ennadai Lake, Keewatin, (61°10'N, 100°55'W) by J. A. Larsen, and from Lynn Lake in Manitoba (56°50'N, 101°03'W) by me. Both deposits lie within the Cockburn end-moraine system, which may represent a late-Wisconsin ice sheet that occupied the Hudson Bay area until at least 8000 years ago (*3*).

Ennadai Lake (Fig. 1) lies at the limit of continuous Boreal forest. Its northern end is in the tundra, while the southern end of the lake is surrounded by an open forest composed mainly of *Picea mariana,* occasional *Picea glauca, Larix laricina, Alnus crispa,* and *Salix spp.* (*4*). The transition from continuous forest to tundra is quite sharp in this area, taking place within about 20 km. Lynn Lake, about 450 km south of Ennadai, lies in an area of open subarctic woodland, where spruce forest dominated by *Picea mariana* constitutes the vegetational climax for the region.

The peat bank at Ennadai Lake is composed primarily of *Sphagnum* bog mosses in varying states of humification. The significance of atmospheric moisture to the growth of *Sphagnum* makes it possible to gain a rough idea of the precipitation-evaporation budget from the rate of *Sphagnum* growth and the degree of humification (or oxidation) of the peat. In northern Europe this concept has resulted in the recognition of wetter and drier episodes from the "recurrence surfaces" and "retardation layers" in the peat bogs (*5*). I suggest

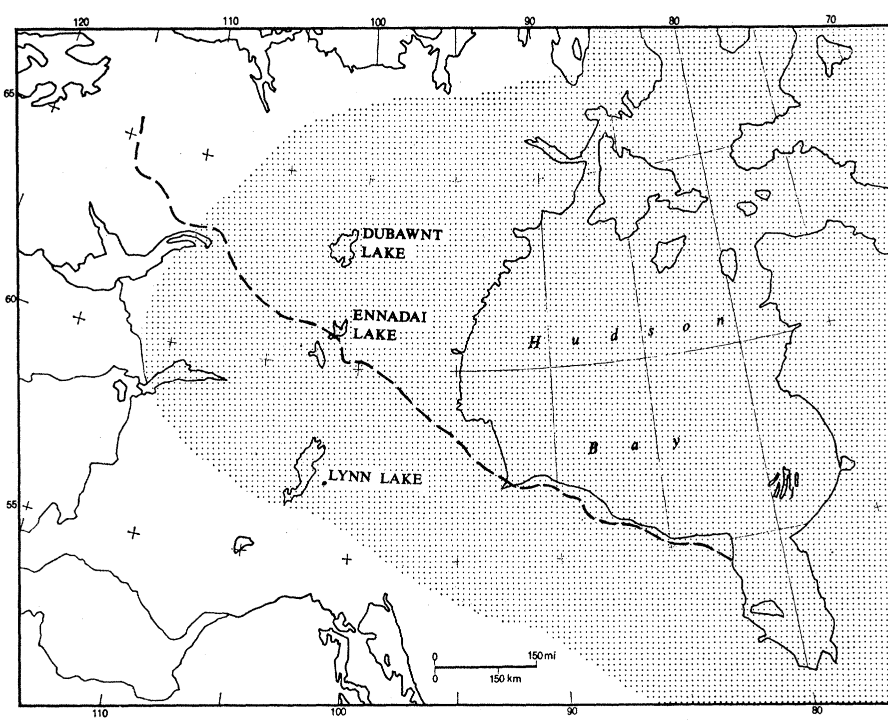

Fig. 1. Location map. The shaded area represents the late Wisconsin ice sheet postulated by Falconer *et al.* (*3*). The broken line depicts the modern limit of continuous forest as mapped by J. A. Larsen (*17*).